MATERIALS CHEMISTRY FRONTIERS

CCS 中国化学会 CHINESE CHEMICAL SOCIETY

ICCAS

ROYAL SOCIETY OF CHEMISTRY

Solvent-Free Isomerization of Heptazine-Trialkoxyl Derivatives Featuring the Efficient Intermolecular Rearrangements

Journal:	*Materials Chemistry Frontiers*
Manuscript ID	QM-RES-03-2025-000246.R1
Article Type:	Research Article
Date Submitted by the Author:	26-May-2025
Complete List of Authors:	Dhara, Barun; RIKEN Center for Emergent Matter Science, Yan, Mengwen; The Chinese University of Hong Kong - Shenzhen, School of Science and Engineering Ibuka, Ryotaro; RIKEN Center for Emergent Matter Science Wang, Jiaxian; The Chinese University of Hong Kong - Shenzhen, School of Science and Engineering Nihonyanagi, Atsuko; RIKEN Center for Emergent Matter Science Inuzuka, Hiroyuki; RIKEN Center for Emergent Matter Science Hamada, Yuko; RIKEN Center for Emergent Matter Science Wakamatsu, Toshie; RIKEN Center for Emergent Matter Science Adachi, Kiyohiro; RIKEN Center for Emergent Matter Science, Materials Characterization Support Team Hashizume, Daisuke; RIKEN Center for Emergent Matter Science, Materials Characterization Support Team Fukui, Norihito; Nagoya University, Department of Molecular and Macromolecular Chemistry, Graduate School of Engineering Miyajima, Daigo; The Chinese University of Hong Kong - Shenzhen, School of Science and Engineering

SCHOLARONE™
Manuscripts

ARTICLE

Solvent-Free Isomerization of Heptazine-Trialkoxyl Derivatives Featuring the Efficient Intermolecular Rearrangements

Received 00th January 20xx,
Accepted 00th January 20xx

DOI: 10.1039/x0xx00000x

Barun Dhara,[a] Mengwen Yan,[b] Ryotaro Ibuka,[a] Jiaxian Wang,[b] Atsuko Nihonyanagi,[a] Hiroyuki Inuzuka[a] Yuko Hamada,[a] Toshie Wakamatsu,[a] Kiyohiro Adachi,[c] Daisuke Hashizume,[c] Norihito Fukui,[d] and Daigo Miyajima[b,a]*

Graphitic carbon nitrides (GCNs) have garnered broad research interest due to their potential in various applications. This study reveals a unique characteristic of heptazine, a repeating structural unit of GCN. Heptazine-trialkoxyl, $Hz(OR)_3$, undergoes nearly quantitative isomerization to trialkylheptazine-trione, $HzTO\text{-}R_3$, under solvent-free conditions. While most of quantitative isomerization proceeds intramolecularly, this isomerization occurs through intermolecular rearrangement reactions. The isomerization introduces three carbonyl groups, drastically altering the physical properties of the parent molecules and making them ideal for stimuli-responsive materials. Since this isomerization proceeds efficiently under solvent-free conditions, it can potentially be integrated into GCN-based materials, offering significant promise for the development of novel GCN-based materials and their applications.

Introduction

Graphitic carbon nitride (GCN) is a graphene-like two-dimensional polymer, composed exclusively of carbon and nitrogen atoms. Since the metal-free photocatalytic properties of GCN were first reported in 2009,[1] researches of GCN have experienced explosive growth.[2-6] Now, its applications have expanded far beyond catalysis, with developments in various areas such as electrode materials leveraging its two-dimensional structure.[7-9] However, challenges remain in achieving uniform synthesis of GCN, and its insolubility in common solvents hampers detailed structural analysis.[10-13] As a result, fundamental properties of GCN have not been fully elucidated in contrast to the remarkable development of its applications. GCN is known to exist in two forms, characterized by repeating structures of heptazine and triazine units, respectively.[14, 15] Recently, the unique properties inherent to these structural units have begun to emerge. Specifically, triazine has been reported to form dynamic covalent bonds based on nucleophilic aromatic substitution (SnAr) reactions,[16, 17] enabling the development of recyclable and malleable thermosets that capitalize on this feature.[18] Meanwhile, our research group successfully synthesized a cyclic triazine trimer—a repeating structural unit of triazine-based GCN—for the first time and reported its exceptional basicity coupled with anion-π interaction.[19] Furthermore, we substantiated unusual photophysical properties in heptazine, where the energetic levels of singlet and triplet excited states are inverted, making it an ideal candidate for OLED light-emitting materials.[20] These newly emerging properties, originated in the conjugated structure of alternating carbon and nitrogen, indicating significant potential for further advancements in GCN-based materials. In this study, we report on the structural isomerization of trialkoxy-heptazine ($Hz(OR)_3$) into trialkylheptazine-trione ($HzTO\text{-}R_3$) that proceeds almost quantitatively under solvent-free conditions (Fig.1). The isomerization progresses independently for each alkoxyl group, and in $Hz(OR)_3$, it takes place consecutively three times, ultimately resulting in the formation of three carbonyl groups in the final isomerized products. Furthermore, detailed experimental analysis unveiled that this isomerization proceeds through intermolecular reactions. Generally, intramolecular reactions tend to proceed faster than intermolecular reactions, with fewer side reactions and higher yields. Notably, despite being an intermolecular reaction, the isomerization of $Hz(OR)_3$ achieves a remarkably high yield. Given its efficient progression

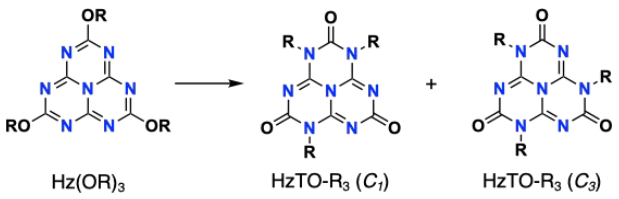

Fig. 1 Schematic illustration of structural isomerization of $Hz(OR)_3$ to $HzTO\text{-}R_3(C_1)$ and $HzTO\text{-}R_3(C_3)$.

[a] RIKEN Center for Emergent Matter Science, 2-1 Hirosawa, Wako, Saitama 351-0198, Japan. E-mail: dmiyajima@cuhk.edu.cn
[b] School of Science and Engineering, the Chinese University of Hong Kong, Shenzhen 518172, P. R. China
[c] Materials Characterization Support Team, RIKEN Center for Emergent Matter Science (CEMS), 2-1 Hirosawa, Wako, Saitama 351-0198, Japan.
[d] Department of Molecular and Macromolecular Chemistry, Graduate School of Engineering, and Integrated Research Consortium on Chemical Science (IRCCS), Nagoya University, Furo-cho, Chikusa-ku, Nagoya, Aichi 464-8603, Japan
† Supplementary Information available: See DOI: 10.1039/x0xx00000x

under solvent-free conditions, this isomerization reaction holds significant promise for the development of stimuli-responsive materials, as well as for further advancements in GCN-based materials.

Results and Discussion

Isomerization is the process by which a molecule is transformed into another molecule with the same chemical formula but a different structure. Since the physical properties of a molecule depend on its structure, if isomerization can be spatiotemporally controlled, it will become a powerful tool for stimuli-responsive materials. Isomerization is classified into structural (constitutional) isomerization and stereoisomerization.[21-24] The former brings about changes in the bonding of functional groups and atoms, while the latter alters the orientation of atoms in three-dimensional space. In the context of stimuli-responsive materials, stereoisomerization is more commonly utilized than structural isomerization. A prominent example is the *cis-trans* isomerization of azobenzene, which undergoes reversible transformations in response to light and heat stimuli.[25, 26] This property has made azobenzene derivatives highly versatile for applications such as film actuators, molecular switches, and optoelectronic smart materials.[25, 27-29] In contrast, structural isomerization, such as the Cope and Claisen rearrangements, are primarily employed as tools in organic synthesis rather than in material design.[30-34] To the best of our knowledge, only proton transfers—specifically excited-state intramolecular proton transfer (ESIPT), which involves the smallest structural changes—are widely utilized in stimuli-responsive materials.[35, 36] This distinction likely arises from the fact that structural isomerization involves bond cleavage and reformation, which restricts its reaction conditions and makes it challenging to integrate into material design. However, isomerization involving significant changes in molecular architecture has the potential to induce substantial alterations in material properties. Therefore, the discovery of large-scale structural isomerization processes applicable to stimuli-responsive materials could significantly advance the field of materials science.

During our previous study,[20] we observed an unusual thermal behaviour in Hz(OR)$_3$. Specifically, when Hz(OBu)$_3$ was characterized using differential scanning calorimetry (DSC) (Fig. 2a), an endothermic peak corresponding to melting was observed at approximately 120 °C, followed by a pronounced exothermic peak at around 240 °C during the first heating process. Notably, no peaks were observed in subsequent heating cycles. However, when Hz(OBu)$_3$ was heated and cooled between 0 °C and 150 °C, the melting/crystallization peaks around 120 °C were consistently observed during both the heating and cooling processes (Fig. S28). This clearly indicates that the exothermic peak observed around 240 °C corresponds to an irreversible change in Hz(OBu)$_3$. Initially, we assumed that Hz(OBu)$_3$ underwent thermal decomposition around 240 °C, leading to the exothermic peak in the DSC chart. However, thermogravimetric analysis (TGA) confirmed that no significant

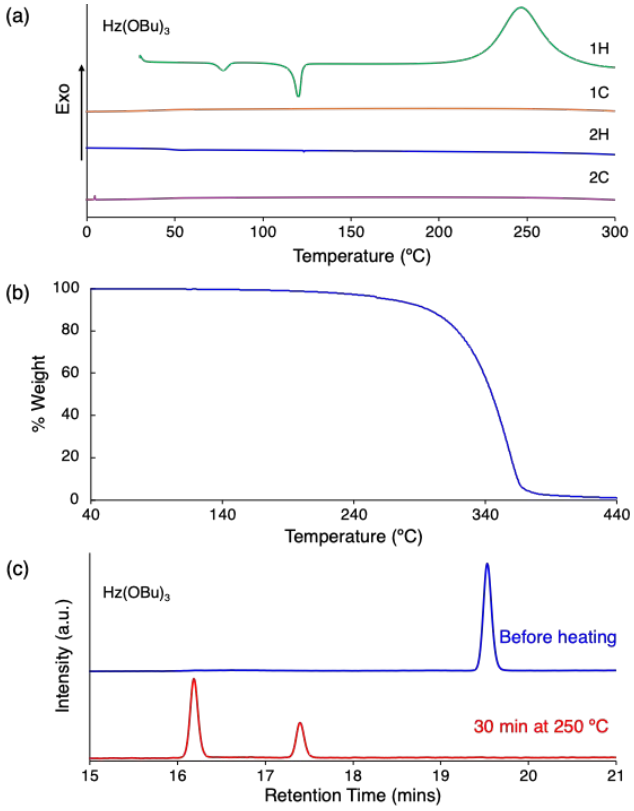

Fig. 2 (a) DSC curves of Hz(OBu)$_3$ obtained at a heating/cooling rate of 10 °C min^{-1}. (b) TGA curve of Hz(OBu)$_3$. (c) LC chromatograms of Hz(OBu)$_3$ before and after heating at 250 °C for 30 minutes.

weight loss occurred below 260 °C (Fig. 2b), ruling out the possibility that the observed exothermic peak results from simple thermal decomposition of Hz(OBu)$_3$ into smaller fragments.

To understand this thermal behaviour, Hz(OBu)$_3$ was heated at 250 °C for 30 min and characterized by liquid chromatography-mass spectrometry (LC-MS) (Fig. 2c). As shown in Fig. 2c, the peak corresponding to the starting material, Hz(OBu)$_3$, disappeared completely, and two new peaks appeared in an approximate 3:1 ratio. Mass spectrometry (MS) revealed that the chemical formula of these new products were identical to the original compound. This strongly suggests that the structural isomerization occurred under solvent-free conditions, resulting in the formation of two structural isomers. Interestingly, after the isomerization, only two peaks were observed in LC chromatogram, and their combined isolation yield exceeded 95% (Supplemental Table 1), indicating that the isomerization proceeded almost quantitatively under solvent-free conditions.

The resultant two isomers were isolated by column chromatography and were characterized by NMR spectroscopy (Figs. S23-S26). ^{1}H and ^{13}C NMR spectra clearly reveal that the product corresponding to the smaller peak in LC chromatogram (Fig.2c) has C_3-symmetry, similar to the starting material, Hz(OBu)$_3$, while the symmetry of the larger appears to be significantly lower than C_3 due to the presence of multiple

This journal is © The Royal Society of Chemistry 20xx

Please do not adjust margins

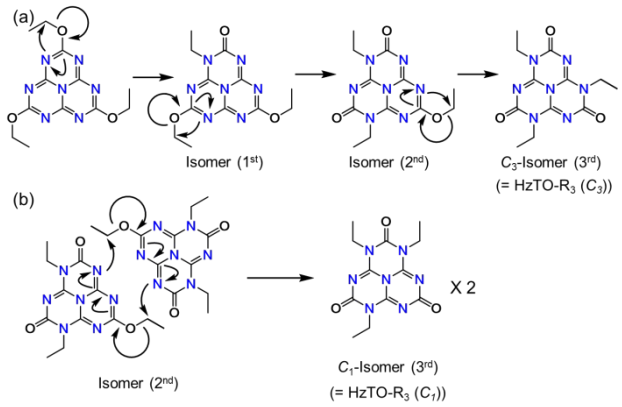

Fig. 3 Proposed (a) intramolecular reaction pathway and (b) representative intermolecular reaction.

peaks. Based on the number of peaks and their chemical shifts, we concluded that $Hz(OBu)_3$ was transformed into two structural isomers, HzTO-Bu_3(C_1) and HzTO-Bu_3(C_3), as depicted in Fig. 1. The labels "C_1" and "C_3" were used to distinguish the two isomers based on their molecular symmetries. The transformation of $Hz(OBu)_3$ into HzTO-R_3(C_1) and HzTO-R_3(C_3) involves the cleavage and reformation of covalent bonds. Initially, based on the high isomerization yield, we hypothesized that the isomerization proceeds via intramolecular rearrangements, as illustrated in Fig. 3a. While this mechanism can explain the formation of the C_3 isomer, it cannot account for the formation of the C_1 isomer. Hence, to explain the formation of the C_1 isomer, we reconsider the possible reaction pathways and propose the intermolecular rearrangement reaction, as shown in Fig. 3b. Here, it is assumed that the reaction proceeds in a concerted manner. However, in this study, the reaction mechanism has not been fully elucidated, and the possibility that the reaction proceeds in a stepwise manner is not ruled out. It is clear that C_1 isomers cannot be formed without intermolecular reactions. To verify that the reaction proceeds intermolecularly, we conducted a control experiment in which two trialkoxy-heptazines with different alkyl chain lengths, $Hz(OPr)_3$ and $Hz(OBu)_3$, were mixed in a 1:1 ratio and heated at 250 °C for 30 minutes. This was done regardless of whether the reaction proceeds via a concerted or a stepwise mechanism. If the isomerization proceeds solely via the intramolecular reactions, this mixed sample would yield four products; HzTO-Pr_3(C_1), HzTO-Pr_3(C_3), HzTO-Bu_3(C_1) and HzTO-Bu_3(C_3). On the other hand, if the isomerization proceeds via intermolecular reactions, twelve kinds of the products would theoretically be synthesized (Fig. 4). As shown in Fig. 4a, the resultant LC chromatogram of the mixed sample displays exactly twelve peaks. With the help of MS analysis, all of the observed peaks

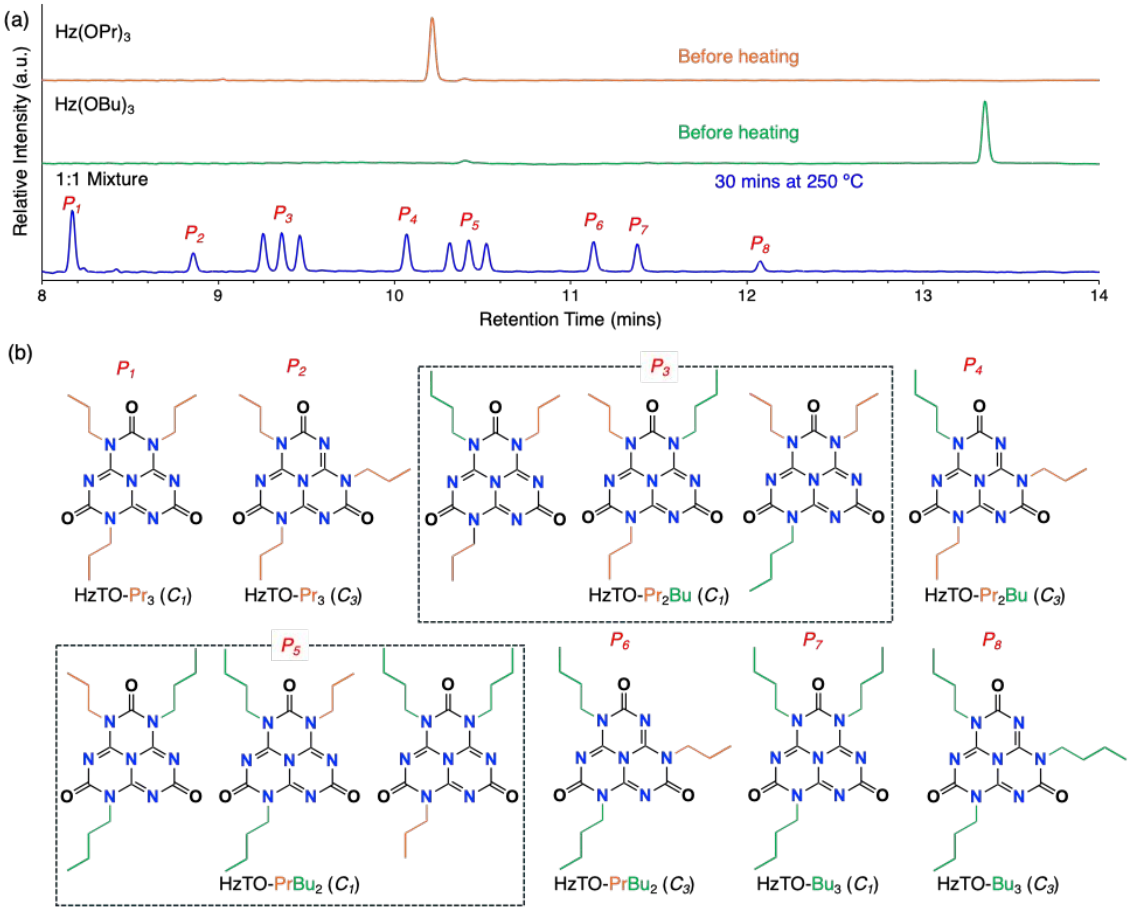

Fig. 4 (a) LC chromatograms of $Hz(OBu)_3$ (green) and $Hz(OPr)_3$ (orange) before heating, and the 1:1 mixture of $Hz(OBu)_3$ and $Hz(OPr)_3$ (blue) after heating at 250 °C for 30 minutes. (b) Molecular structures assigned to the peaks observed in (a).

Please do not adjust margins

were assigned to these twelve isomers (Fig. S33-1 – S33-8). Hence, it is evident that the isomerization of $Hz(OR)_3$ proceeds via intermolecular reactions. However, this result alone cannot exclude the possibility that intramolecular reaction occur alongside the intermolecular reaction. To address this, $Hz(OBu)_3$ was heated under the dilute conditions in toluene at 250°C (under high pressure) for 30 minutes but no reaction occurred, indicating that the intramolecular reaction, as depicted in Fig. 3a, is not involved. Therefore, we conclude that the observed isomerization proceeds exclusively via the intermolecular reaction mechanism.

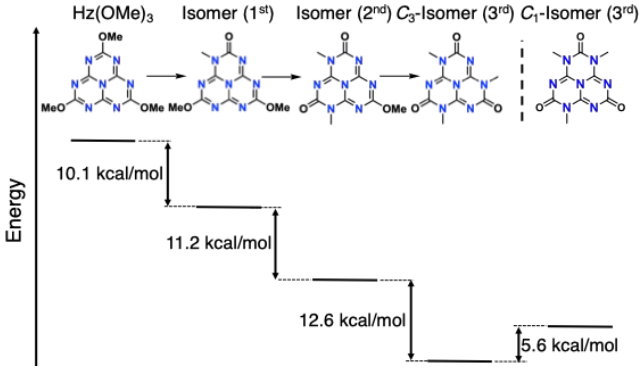

Fig. 5 Energy diagram of $Hz(OMe)_3$ and its corresponding structural isomers.

Next, we investigated the driving force behind this isomerization using DFT calculations (Fig. 5). Since the chemical formula of the isomers are identical, it is possible to directly compare their thermodynamic stabilities. The thermal free energies at 298 K were estimated by DFT calculations at the B3LYP/6-31G(d) level. As a result, it was revealed that the thermodynamic stability increases as the isomerization proceeds. This increased stability is attributed to the formation of carbonyl groups, which is known as the thermodynamically stable functional groups. On the other hand, the DFT calculations indicate that C_3 isomer is more stable than C_1 isomer by 5.6 kcal/mol. However, the yield of C_1 isomer is almost three times larger than that of C_3 isomer. As discussed in Supplementary Note (1), if the alkyl chain transfer occurs randomly without positional selectivity, C_1 and C_3 isomers are formed in 3:1 ratio statistically, which is consistent with the observed HPLC results. Hence, we concluded that the intermolecular rearrangements occur randomly under the conditions employed in this study. For our curiosity, we extended the reaction time to 24 hours at 250 °C, while C_1 isomer was not converted into C_3 isomer. Interestingly, a detailed analysis of this energy difference reveals that the degree of stabilization achieved from each isomerization increases as the reaction progresses from the first to the second and then to the third step (Fig. 5). This suggests that the second isomerization is more likely to occur than the first, and the third isomerization is even more likely to occur than the second. To support this assumption, $Hz(OBu)_3$ was heated at a lower temperature, 150 °C (Fig. 6). After heating at 150 °C for 12 hours, two new peaks were observed alongside the isomerized products, but these peaks nearly disappeared after 36 hours, indicating that they are intermediates of the isomerization into HzTO-Bu_3(C_1) and HzTO-Bu_3(C_3) (like isomer(1st) and isomer (2nd) in Fig. 3a). Interestingly, although the starting material, $Hz(OBu)_3$, still remained after 24 hours, the sum of the peak integration of these two intermediates was smaller than that of the fully isomerized products. This observation aligns well with the results of DFT calculations, suggesting that once the isomerization begins, it is strongly driven to completion, which accounts for the high yield and the minimal observation of intermediates. We also conducted similar isomerization experiments using $Hz(OMe)_3$, $Hz(OEt)_3$, and $Hz(OPr)_3$ and confirmed the similar quantitative isomerizations (See DSC, TGA, LC chromatograms and isolation yields in Supplementary Information). On the other hand, regardless of temperature, $Hz(OiPr)_3$ consistently produced byproducts resulting from the loss of one or two alkyl chains (Fig. S34). Since the elimination of the alkyl chain was more frequently observed in the case of the secondary alcohol, isopropanol, we propose that this elimination reaction proceeds via the E2 mechanism. In the case of $Hz(OR)_3$ with tertiary alcohols, the same side reaction is more likely to occur. It is worth noting that, in the case of $Hz(OBu)_3$, side products resulting from the loss of one alkyl chain were also occasionally observed. However, such side reaction was suppressed by increasing the temperature and

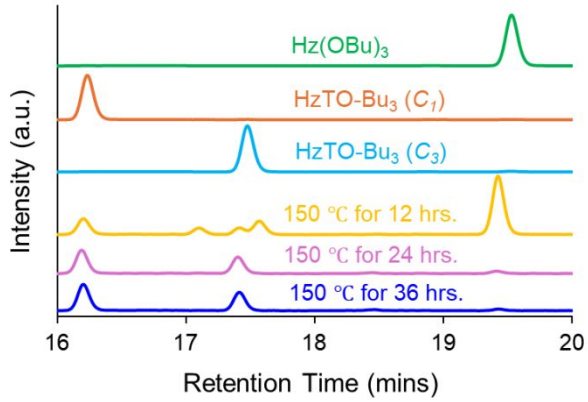

Fig. 6 LC chromatograms of $Hz(OBu)_3$ (green), HzTO-Bu_3(C_1) (orange), and HzTO-Bu_3(C_3) (cyan). Time-dependent HPLC analysis of $Hz(OBu)_3$ heated at 150 °C for different time; 12 hours (yellow), 24 hours (magenta), and 36 hours (blue).

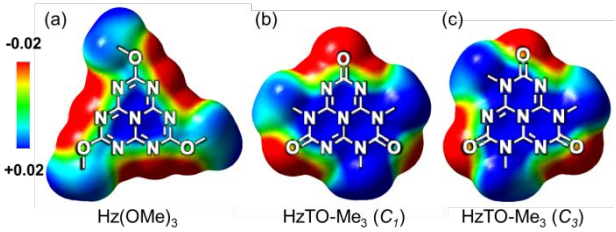

Fig. 7 Electrostatic potential maps for (a) $Hz(OMe)_3$, (b) HzTO-Me_3 (C_3) and (c) HzTO-Me_3 (C_1).

This journal is © The Royal Society of Chemistry 20xx

Please do not adjust margins

replacing the atmosphere with nitrogen. Hence, we assume that the E2 reaction is accelerated by the presence of water molecules.

For the application of the isomerization in stimuli-responsive materials, significant changes in physical properties accompanying the isomerization are highly desirable. Hence, we scrutinized the changes before and after the isomerization. The first noticeable, big change is the introduction of three carbonyl groups. Carbonyl groups are polar and are known to form dipole-dipole interactions and hydrogen bondings.[37] In fact, when calculating and comparing electron density maps, it is evident that electron density is initially equally localized on the peripheral oxygens and nitrogens, but shifts to the carbonyl oxygens after isomerization (Fig. 7). Before isomerization, $Hz(OR)_3$ also contains three ether oxygens, but their polarity is relatively low, and they form much weaker intermolecular interactions compared to carbonyl oxygens.[37] This assumption is supported by the observation that the melting temperatures of isomerized products, HzTO-Et_3(C_1) and HzTO-Et_3(C_3) are higher than that of $Hz(OEt)_3$ by 70 °C. Similarly, regardless of the length of their alkyl chains, the melting temperatures increased after isomerization in all cases (Fig. S29). To understand the origin of the enhanced intermolecular interaction between the isomerized products, we attempted to characterize the single crystal structures of the isomerized products and successfully solved some of them with shorter alkyl chains such as HzTO-Me_3(C_1), HzTO-Me_3(C_3), HzTO-Et_3(C_1), HzTO-Et_3(C_3), HzTO-Pr_3(C_1), and HzTO-Pr_3(C_3). As illustrated in Fig. 8 and Fig.S37-S42,

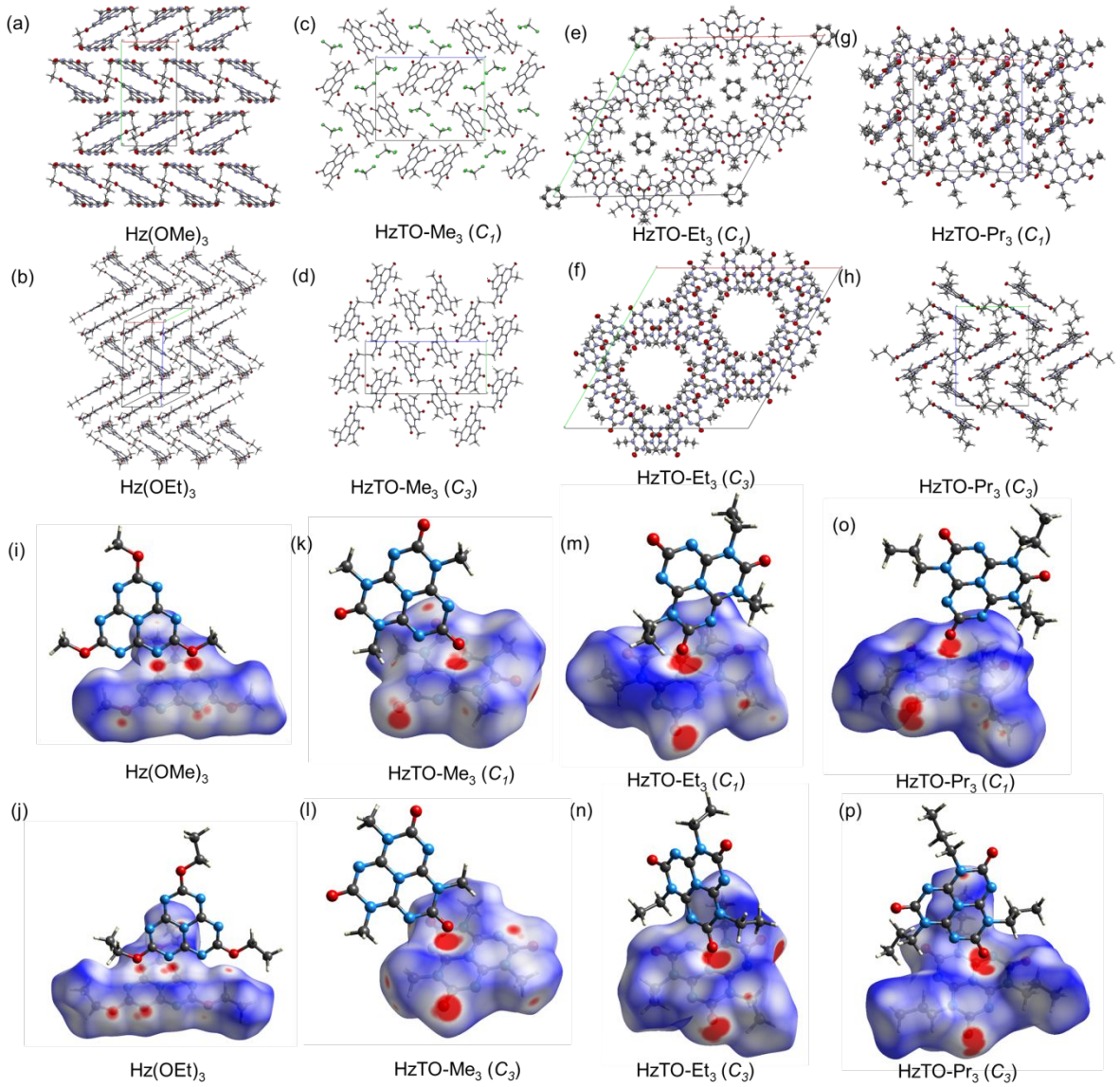

Fig.8 Crystal structures of $Hz(OMe)_3$ (a), $Hz(OEt)_3$ (b), HzTO-Me_3(C_1) (c), HzTO-Me_3(C_3) (d), HzTO-Et_3(C_1) (e), HzTO-Et_3(C_3) (f), HzTO-Pr_3(C_1) (g), and HzTO-Pr_3(C_3) (h), blue, red, black, green, and white sphere represented nitrogen, oxygen, carbon, chlorine, and hydrogen respectively. Hirshfeld surface analysis (d_{norm}) of $Hz(OMe)_3$ (i), $Hz(OEt)_3$ (j), HzTO-Me_3(C_1) (k), HzTO-Me_3(C_3) (l), HzTO-Et_3(C_1) (m), HzTO-Et_3(C_3) (n), HzTO-Pr_3(C_1) (o), and HzTO-Pr_3(C_3) (p). Close intermolecular contacts are highlighted in red, indicating regions of strong interactions, while weaker or more distant interactions transition from white to blue.

Please do not adjust margins

the resultant packing structures differ significantly depending on the different lengths of alkyl chains. Furthermore, HzTO-Me_3(C_3), HzTO-Et_3(C_1), and HzTO-Et_3(C_3) were obtained as co-crystals with solvent molecules. However, despite these differences, we identified a common feature in all these crystals in their Hirshfeld surface profiles.[38] In Hirshfeld surface profiles, red and blue regions correspond to shorter and longer contacts than van der Waals interactions, respectively. As shown in Fig. 8c–h, all six isomerized products form strong intermolecular interactions between the oxygen and π-plane in a similar manner, indicating that this carbonyl-π interaction plays an important role in determining their packing structures. On the other hand, we also successfully solved the single crystal structures of $Hz(OMe)_3$ and $Hz(OEt)_3$ (Fig. 8 and Fig. S43). Their Hirshfeld surface profiles revealed that both nitrogen and oxygen simultaneously form relatively strong intermolecular interaction with the π-plane in a similar manner between the two crystals, although their packing arrangements themselves are different. As mentioned earlier, due to the low polarity of ether oxygens, we concluded that, in contrast to the carbonyl oxygens in the isomerized products, both nitrogen and oxygen need to interact cooperatively to form relatively stable interactions. To support this assumption, we further characterized the single crystals of $Hz(OMe)_3$, HzTO-Me_3(C_1), HzTO-Me_3(C_3) using natural bond analysis (NBO).[39] NBO analysis allows for the identification and quantification of intermolecular interactions. As summarized in Fig. S45-S47, NBO analysis revealed that the interactions highlighted in red on the Hirshfeld surface profiles are electrostatic/charge-transfer interactions between lone pairs of oxygen/nitrogen and the anti-bonding orbital of the C-N bond in all three cases. The magnitude of these interactions was shown to be much larger for carbonyl oxygen, supporting the above hypothesis. It is clear that the introduction of highly polar carbonyl groups indeed brings significant changes to intermolecular interactions.

Finally, we compare this study with related studies. To the best of our knowledge, no similar isomerization of heptazines has been reported. However, the tautomerization of $Hz(OH)_3$ to HzTO-H_3 were already reported.[40, 41] The equilibrium of this tautomerization is biased to HzTO-H_3, but it is known that the addition of a strong base, such as KOH, can revert it back to the potassium salt of $Hz(OH)_3$, $Hz(OK)_3$,[40] while the isomerization of $Hz(OR)_3$ to HzTO-R_3 is irreversible. During our literature search, we noticed that a similar type of isomerization has been reported for triazine trioxyalkyl ($Tz(OR)_3$).[42-44] More than 45 years have passed since the first report on the isomerization of $Tz(OR)_3$, but the number of literatures reporting on this isomerization is still fewer than 20. (See Supplementary Note(2)). Furthermore, no detailed discussions on its isomerization mechanism have been reported. In the case of triazines, only a single type (C_3-sym) of product is formed during isomerization, which has likely led to the assumption that the reaction proceeds via intramolecular rearrangement reactions. To verify the reaction mechanism, we mixed $Tz(OEt)_3$ and $Tz(OPr)_3$ in a 1:1 ratio and heated the mixture at 250 °C for 1 hour. Gas chromatography-mass spectrometry (GC-MS) analysis revealed the presence of products consisting of two different alkyl chains, leading to the conclusion that the isomerization of $Tz(OR)_3$ also proceeds via the intermolecular reaction mechanism (Fig. S35-S36).[42]

Conclusions

In this study, we have reported the unique isomerization exhibited by heptazines and elucidated its reaction mechanism. Although a similar type of isomerization had been reported for $Tz(OR)_3$, it was not self-evident whether the same isomerization would proceed in the larger π-conjugated system of heptazine. Both triazine and heptazine are recognized as repeating structural units of GCNs. Because it is relatively easy to combine this isomerization into GCN-based materials, this study will contribute not only to heptazine-based materials but also to the broader field of GCN-based materials.

Author contributions

D.M. conceived and supervised the research project. B.D., R.I., M.Y., J.W., and A.N. performed the isomerization experiments. H.I., Y.H., and R.I. conducted the LC-MS analysis. T.W. carried out the DSC and TGA analyses. B.D., K.A., and D.H. performed the X-ray analysis. N.F. and B.D. conducted the computational calculations. D.M. and B.D. wrote the manuscript, and all authors reviewed and approved the final version.

Conflicts of interest

The authors declare no conflict of interest.

Data availability

Supporting information contains materials and methods, synthetic procedures, experimental details, NMR, Mass, UV-absorption, DSC, TGA, crystallographic data of compounds and theoretical calculations.

CCDC 2420172, 2420173, 2420174, 2420175, 2420176, 2420177, 2420178, 2420086, and 2420087 contain the supplementary crystallographic data for this paper. These data can be obtained free of charge via www.ccdc.cam.ac.uk/data_request/cif, or by emailing data_request@ccdc.cam.ac.uk, or by contacting The Cambridge Crystallographic Data Centre, 12 Union Road, Cambridge CB2 1EZ, UK; fax:+441223336033.

Acknowledgements

This study was supported by JST PRESTO (Grant No. JP1159382), Shenzhen Science and Technology Program (Grant No. 2024SC0019), and the Guangdong Basic Research Center of Excellence for Aggregate Science and the National Natural Science Foundation of China (Grant No. 52272056). We are thankful to Toshihiko Nogawa for analyzing the liquid

This journal is © The Royal Society of Chemistry 20xx

Please do not adjust margins

chromatography mass spectra (LC-MS), which were acquired at the Mass Spectrometry Facility, Molecular Structure Characterization Unit, RIKEN CSRS.

Notes and references

1. X. Wang, K. Maeda, A. Thomas, K. Takanabe, G. Xin, J. M. Carlsson, K. Domen and M. Antonietti, *A metal-free polymeric photocatalyst for hydrogen production from water under visible light*, *Nat. Mater.*, 2009, **8**, 76-80.
2. S. C. Yan, Z. S. Li and Z. G. Zou, *Photodegradation Performance of g-C3N4 Fabricated by Directly Heating Melamine*, *Langmuir : the ACS journal of surfaces and colloids*, 2009, **25**, 10397-10401.
3. J. Liu, T. Zhang, Z. Wang, G. Dawson and W. Chen, *Simple pyrolysis of urea into graphitic carbon nitride with recyclable adsorption and photocatalytic activity*, *J. Mater. Chem.*, 2011, **21**, 14398-14401.
4. Y. Wang, X. Wang and M. Antonietti, *Polymeric Graphitic Carbon Nitride as a Heterogeneous Organocatalyst: From Photochemistry to Multipurpose Catalysis to Sustainable Chemistry*, *Angew. Chem. Int. Ed.*, 2012, **51**, 68-89.
5. J. Liu, Y. Liu, N. Liu, Y. Han, X. Zhang, H. Huang, Y. Lifshitz, S.-T. Lee, J. Zhong and Z. Kang, *Metal-free efficient photocatalyst for stable visible water splitting via a two-electron pathway*, *Science*, 2015, **347**, 970-974.
6. M. Singhal, S. Jangir, S. Upadhyay and D. S. Rajawat, *Advances in graphitic carbon nitride: a comprehensive review of synthesis, properties, applications and recent developments with photoelectrochemical water splitting*, *Discov. Chem.*, 2024, **1**, 64.
7. J. Safaei, N. A. Mohamed, M. F. Mohamad Noh, M. F. Soh, N. A. Ludin, M. A. Ibrahim, W. N. Roslam Wan Isahak and M. A. Mat Teridi, *Graphitic carbon nitride (g-C_3N_4) electrodes for energy conversion and storage: a review on photoelectrochemical water splitting, solar cells and supercapacitors*, *J. Mater. Chem. A*, 2018, **6**, 22346-22380.
8. Y. Chen and C. Lu, *Graphitic carbon nitride nanomaterials for high-performance supercapacitors*, *Carbon Neutralization*, 2023, **2**, 585-602.
9. A. O. Idris, E. O. Oseghe, T. A. M. Msagati, A. T. Kuvarega, U. Feleni and B. Mamba, *Graphitic Carbon Nitride: A Highly Electroactive Nanomaterial for Environmental and Clinical Sensing*, *Sensors*, 2020, **20**, 5743.
10. H. Arazoe, D. Miyajima, K. Akaike, F. Araoka, E. Sato, T. Hikima, M. Kawamoto and T. Aida, *An autonomous actuator driven by fluctuations in ambient humidity*, *Nat. Mater.*, 2016, **15**, 1084-1089.
11. G. Algara-Siller, N. Severin, S. Y. Chong, T. Björkman, R. G. Palgrave, A. Laybourn, M. Antonietti, Y. Z. Khimyak, A. V. Krasheninnikov, J. P. Rabe, U. Kaiser, A. I. Cooper, A. Thomas and M. J. Bojdys, *Triazine-Based Graphitic Carbon Nitride: a Two-Dimensional Semiconductor*, *Angew. Chem. Int. Ed.*, 2014, **53**, 7450-7455.
12. X. Zhang, X. Zhang, P. Yang and S. P. Jiang, *Layered graphitic carbon nitride: nano-heterostructures, photo/electro-chemical performance and trends*, *J. Nanostruct. Chem.*, 2022, **12**, 669-691.
13. M. Y. Akram, T. Ashraf, L. Tong, X. Yin, H. Dong and H. Lu, *Architecting high-performance photocatalysts: A review of modified 2D/2D graphene/g-C_3N_4 heterostructures*, *J. Environ. Chem. Eng.*, 2024, **12**, 113415.
14. Y. Li, F. Gong, Q. Zhou, X. Feng, J. Fan and Q. Xiang, *Crystalline isotype heptazine-/triazine-based carbon nitride heterojunctions for an improved hydrogen evolution*, *Applied Catalysis B: Environmental*, 2020, **268**, 118381.
15. B. V. Lotsch, M. Döblinger, J. Sehnert, L. Seyfarth, J. Senker, O. Oeckler and W. Schnick, *Unmasking Melon by a Complementary Approach Employing Electron Diffraction, Solid-State NMR Spectroscopy, and Theoretical Calculations—Structural Characterization of a Carbon Nitride Polymer*, *Chem. - Eur. J.*, 2007, **13**, 4969-4980.
16. Z. Lei, L. J. Wayment, J. R. Cahn, H. Chen, S. Huang, X. Wang, Y. Jin, S. Sharma and W. Zhang, *Cyanurate-Linked Covalent Organic Frameworks Enabled by Dynamic Nucleophilic Aromatic Substitution*, *J. Am. Chem. Soc.*, 2022, **144**, 17737-17742.
17. Z. Lei, Z. Wang, H. Jiang, J. R. Cahn, H. Chen, S. Huang, Y. Jin, X. Wang, K. Yu and W. Zhang, *Dual-Factor-Controlled Dynamic Precursors Enable On-Demand Thermoset Degradation and Recycling*, *Adv. Mater.*, 2024, **36**, 2407854.
18. Z. Lei, H. Chen, C. Luo, Y. Rong, Y. Hu, Y. Jin, R. Long, K. Yu and W. Zhang, *Recyclable and malleable thermosets enabled by activating dormant dynamic linkages*, *Nat. Chem.*, 2022, **14**, 1399-1404.
19. H. Gong, C. Zhang, T. Ogaki, H. Inuzuka, D. Hashizume and D. Miyajima, *Azacalix[3]triazines: A Substructure of Triazine-Based Graphitic Carbon Nitride Featuring Anion-π Interactions*, *Angew. Chem. Int. Ed.*, 2021, **60**, 16377-16381.
20. N. Aizawa, Y. J. Pu, Y. Harabuchi, A. Nihonyanagi, R. Ibuka, H. Inuzuka, B. Dhara, Y. Koyama, K. I. Nakayama, S. Maeda, F. Araoka and D. Miyajima, *Delayed fluorescence from inverted singlet and triplet excited states*, *Nature*, 2022, **609**, 502-506.
21. M. L. v. Frenkel', *Thermodynamic properties of isomerization reactions*, CRC Press, 2020.
22. G. P. Moss, *Basic terminology of stereochemistry (IUPAC Recommendations 1996)*, *Pure and Applied Chemistry*, 1996, **68**, 2193-2222.
23. J. D. Roberts, M. C. Caserio and J. D. Roberts, *Basic principles of organic chemistry*, WA Benjamin New York, 1965.
24. P. Kalsi, *Stereochemistry conformation and mechanism*, New Age International, 2005.
25. H. M. D. Bandara and S. C. Burdette, *Photoisomerization in different classes of azobenzene*, *Chem. Soc. Rev.*, 2012, **41**, 1809-1825.
26. G. S. Hartley, *The Cis-form of Azobenzene*, *Nature*, 1937, **140**, 281-281.
27. L. W. Giles, C. F. J. Faul and R. F. Tabor, *Azobenzene isomerization in condensed matter: lessons for the design of efficient light-responsive soft-matter systems*, *Mater. Adv.*, 2021, **2**, 4152-4164.
28. A. H. Gelebart, D. Jan Mulder, M. Varga, A. Konya, G. Vantomme, E. W. Meijer, R. L. B. Selinger and D. J. Broer, *Making waves in a photoactive polymer film*, *Nature*, 2017, **546**, 632-636.
29. M. Younis, S. Ahmad, A. Atiq, M. Amjad Farooq, M. H. Huang and M. Abbas, *Recent Progress in Azobenzene-Based Supramolecular Materials and Applications*, *Chem Rec*, 2023, **23**, e202300126.
30. R. P. Lutz, *Catalysis of the Cope and Claisen rearrangements*, *Chem. Rev.*, 1984, **84**, 205-247.
31. J. J. Gajewski, *Hydrocarbon thermal isomerizations*, Elsevier, 2004.
32. H. Ito, A. Sato and T. Taguchi, *Enantioselective aromatic Claisen rearrangement*, *Tetrahedron Lett.*, 1997, **38**, 4815-4818.

33. M. J. S. Dewar and L. E. Wade, Jr., *A study of the mechanism of the Cope rearrangement*, *J. Am. Chem. Soc.*, 1977, **99**, 4417-4424.
34. A. M. Martín Castro, *Claisen Rearrangement over the Past Nine Decades*, *Chem. Rev.*, 2004, **104**, 2939-3002.
35. P.-Y. Fu, S.-Z. Yi, M. Pan and C.-Y. Su, *Excited-State Intramolecular Proton Transfer (ESIPT) Based Metal–Organic Supramolecular Optical Materials: Energy Transfer Mechanism and Luminescence Regulation Strategy*, *Acc. Mater. Res.*, 2023, **4**, 939-952.
36. W. Wang, M. Marshall, E. Collins, S. Marquez, C. Mu, K. H. Bowen and X. Zhang, *Intramolecular electron-induced proton transfer and its correlation with excited-state intramolecular proton transfer*, *Nat. Commun.*, 2019, **10**, 1170.
37. F. H. Allen, C. A. Baalham, J. P. M. Lommerse and P. R. Raithby, *Carbonyl–Carbonyl Interactions can be Competitive with Hydrogen Bonds*, *Acta Cryst. B*, 1998, **B54**, 320-329.
38. M. A. Spackman and D. Jayatilaka, *Hirshfeld surface analysis*, *CrystEngComm*, 2009, **11**, 19-32.
39. A. E. Reed, L. A. Curtiss and F. Weinhold, *Intermolecular interactions from a natural bond orbital, donor-acceptor viewpoint*, *Chem. Rev.*, 1988, **88**, 899-926.
40. N. E. A. El-Gamel, L. Seyfarth, J. Wagler, H. Ehrenberg, M. Schwarz, J. Senker and E. Kroke, *The Tautomeric Forms of Cyameluric Acid Derivatives*, *Chem. Eur. J.*, 2007, **13**, 1158-1173.
41. E. Kroke, M. Schwarz, E. Horath-Bordon, P. Kroll, B. Noll and A. D. Norman, *Tri-s-triazine derivatives. Part I. From trichloro-tri-s-triazine to graphitic C3N4 structures*, *New J. Chem.*, 2002, **26**, 508-512.
42. V. R. Likhterov, S. V. Klenovich, V. S. étlis, L. A. Tsareva, é. G. Pomerantseva and S. M. Shmuilovich, *Inter- and intramolecular rearrangements of cyanuric acid triallyl esters*, *Chem. Heterocycl. Compd.*, 1988, **24**, 308-311.
43. M. L. Tosato, *Methyltropic tautomerism of the N–C–O and N–C–S groups: synthesis of methyl mono- and di-thiocyanurates*, *J. Chem. Soc., Perkin Trans. 2*, 1979, DOI: 10.1039/P29790001371, 1371-1375.
44. M. Kaftory and E. Handelsman-Benory, *Thermal Rearrangement of Cyanurates in the Solid State*, *Mol. Cryst. Liq. Cryst*, 1994, **240**, 241-249.

This journal is © The Royal Society of Chemistry 20xx

Please do not adjust margins

Supporting information contains materials and methods, synthetic procedures, experimental details, NMR, Mass, UV-absorption, DSC, TGA, crystallographic data of compounds and theoretical calculations.

CCDC 2420172, 2420173, 2420174, 2420175, 2420176, 2420177, 2420178, 2420086, and 2420087 contain the supplementary crystallographic data for this paper. These data can be obtained free of charge via www.ccdc.cam.ac.uk/data_request/cif, or by emailing data_request@ccdc.cam.ac.uk, or by contacting The Cambridge Crystallographic Data Centre, 12 Union Road, Cambridge CB2 1EZ, UK; fax:+441223336033.